CHEMISTRY OF MATERIALS
Cite This: Chem. Mater. 2018, 30, 1849−1855
Article
pubs.acs.org/cm

Molecule-Adsorbed Topological Insulator and Metal Surfaces: A Comparative First-Principles Study

Soumyajit Sarkar,[†] Jing Yang,[‡] Liang Z. Tan,[‡] Andrew M. Rappe,[‡] and Leeor Kronik*[,†]

[†]Department of Materials and Interfaces, Weizmann Institute of Science, Rehovoth 76100, Israel
[‡]Department of Chemistry, University of Pennsylvania, Philadelphia, Pennsylvania 19104-6323, United States

Supporting Information

ABSTRACT: We compare electronic structure characteristics of three different kinds of benzene-adsorbed (111) surfaces: that of Bi_2Te_3, a prototypical topological insulator, that of Au, a prototypical inert metal, and that of Pt, a prototypical catalytic metal. Using first-principles calculations based on dispersion-corrected density functional theory, we show that benzene is chemisorbed on Pt, but physisorbed on Au and Bi_2Te_3. The adsorption on Bi_2Te_3 is particularly weak, consistent with a minimal perturbation of the electronic structure at the surface of the topological insulator, revealed by a detailed analysis of the interaction of the molecular orbitals with the topological surface states.

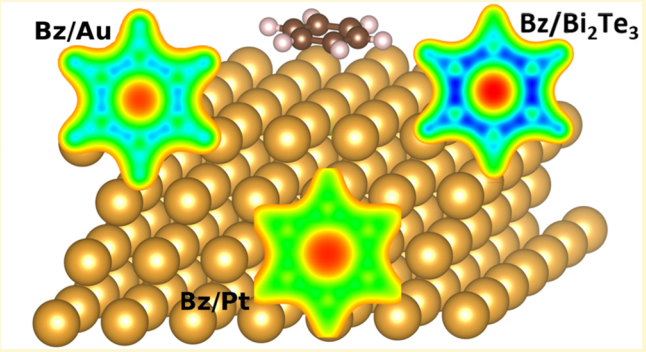

INTRODUCTION

Topological insulators (TIs) are a newly identified class of solids,[1,2] in which strong spin−orbit coupling (SOC) leads to a state of matter which is distinct from ordinary ("trivial") insulators. Even though in both trivial and topological insulators electrons cannot conduct in the bulk, TI surfaces support metallic electronic states that are "protected" by constraints of time-reversal symmetry.[3−7] These metallic surface states are unique in that they exhibit spin-momentum locking, and electron backscattering from them is suppressed, requiring a spin flip. Metallic surface states at TI surfaces also differ from surface states at conventional metal surfaces in that they arise in an otherwise forbidden gap, whereas in a metal the consequences of surface states can be (and close to the surface often are) overwhelmed by the density of evanescent metallic bulk states at the surface.[8]

One way to modify surface electronic properties, which has been studied extensively, is via the adsorption of molecules (see, e.g., refs 9−19). Generally, molecule adsorption allows one to harness the power and flexibility of organic chemistry to tailor desired surface properties. Extensive research has shown that this is indeed possible and, furthermore, often results in novel collective effects emerging from various forms of molecule−surface interaction (see, e.g., refs 20−26). With this in mind, recent years have seen several important studies of the effect of molecular adsorption on TI surfaces.[27−33] While some studies[30,33] emphasized surface protection by an organic overlayer, most of this effort has been focused on the interaction of TI surfaces with magnetic molecules, especially phthalocyanines. This is important because the interaction of magnetic molecules with ordinary metallic surfaces has already been shown to result in unusual magnetic effects[26,34−37] and because magnetic impurities break the time-reversal symmetry protecting TI surfaces.

The topologically protected nature of states at the TI surface has also triggered suggestions for a broad range of applications,[38] including heterogeneous catalysis.[39−41] It is therefore of particular interest to study how the surface states of a TI interact with the energy levels of an adsorbed molecule and how this may affect the electronic structure at the interface. To the best of our knowledge, so far only little work[27,32] has been devoted to understanding the consequences of the unique TI surface states for the molecule−surface state interaction. Here, we wish to compare and contrast molecule−TI and molecule−metal interactions from first-principles, using density functional theory (DFT). We consider modifications in the electronic structure brought about by the adsorption of benzene, a simple closed-shell prototypical organic molecule, on Bi_2Te_3 (a prototypical TI), Au (a prototypical inert metal), and Pt (a prototypical catalytic metal). We find that benzene adsorption on Bi_2Te_3 is significantly weaker than on the metallic surfaces, consistent with a minimal perturbation of the electronic structure at the surface of the topological insulator, revealed by a detailed analysis of the interaction of the molecular orbitals with the topological surface states.

COMPUTATIONAL DETAILS

All DFT calculations were performed within the generalized-gradient approximation (GGA) using the Perdew−Burke−Ernzerhof (PBE) functional.[42] In order to account for the beznene−substrate dispersive

Received: July 27, 2017
Revised: February 24, 2018
Published: February 25, 2018

DOI: 10.1021/acs.chemmater.7b03176
Chem. Mater. 2018, 30, 1849−1855

interaction, we have augmented the PBE functional with the surface-screened version[43] of the Tkatchenko–Scheffler[44] pairwise dispersive correction, which we denote as PBE+TS^{surf}. All calculations were performed using the VASP code,[45] a plane-wave code, in which ion–electron interactions are treated with the projector augmented wave (PAW) approach.[46,47] A kinetic energy cutoff of 550 eV was used for plane-wave basis set expansion. Spin–orbit coupling was explicitly included in all calculations, as implemented within the PAW method in the VASP code.[48]

The Bi_2Te_3(111) surface was represented using a 4 × 4 supercell containing a slab that comprises four quintuple layer (QL) units, each of which consists of alternating Bi and Te layers, as shown in Figure 1.[49] In each atomic layer, the atoms form a triangular lattice such that

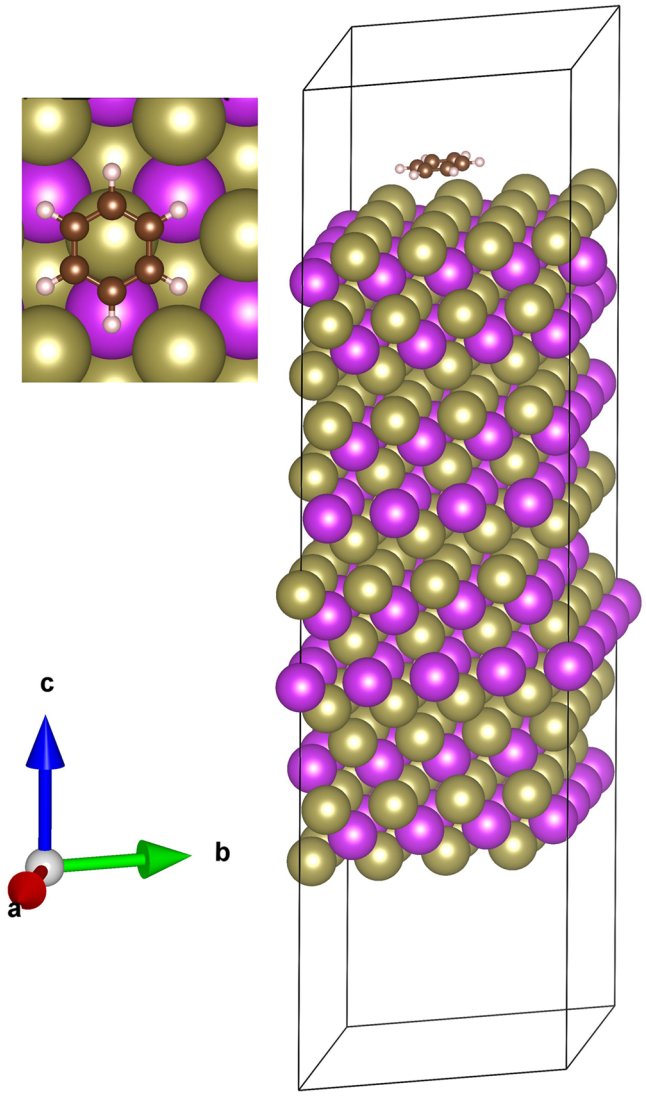

Figure 1. Unit cell of four quintuple layers of Bi_2Te_3 with a single adsorbed benzene molecule. Bi, Te, C, and H atoms are represented by magenta, gray, brown, and pink balls, respectively. Inset: top view of the position and orientation of the benzene molecule on the top surface.

their in-plane positions are commensurate with the (111) surface of a face-centered-cubic lattice. Together with the adsorbed benzene molecule, the supercell contains 332 atoms. Atoms of the benzene molecule and the two topmost QLs were allowed to relax until forces smaller than 5 meV/Å were obtained, with all other atoms fixed at their bulk positions. Au and Pt (111) surfaces were represented using a 6 × 6 supercell containing a slab comprising four layers. Atoms of the benzene molecule and all metal atoms except those of the bottom-most layer were allowed to relax until forces smaller than 5 meV/Å were obtained, with all other atoms fixed at their bulk position. A 4 × 4 × 1 Monkhorst–Pack[50] k-point mesh was used for Brillouin zone integration.

In order to identify the TI surface bands, each wave function at a given energy band and $\vec{k}_{\|}$ (momentum parallel to the surface) was projected onto spherical harmonics around each ion.[51] TI surface bands were identified based on a 60% critical percentage of the projections onto the three top (or bottom) layers of the surface. The threshold value was chosen such that the surface states identified within the energy window do not change significantly with the variation of the given threshold.[52]

RESULTS AND DISCUSSION

We find the optimized faced-centered-cubic (FCC) lattice parameters of Au and Pt to be 4.15 and 3.94 Å, respectively. These values are in good agreement with past theory and experiment.[53] Using these lattice parameters, we constructed a supercell containing four layers along the (111) direction and 20 Å of vacuum normal to the surface, for each system. For these metallic slabs, a 6 × 6 supercell in the *xy* plane was used so as to approach the low-coverage limit of a single benzene molecule adsorbed on each surface. For Bi_2Te_3, the optimal lattice constants were found to be $a = b = c = 10.46$ Å and $\alpha = \beta = \gamma = 20.05°$, consistent with past theoretical and experimental reports.[52,54]

We first consider the molecule-adsorbed transition metal surfaces, Bz/Pt(111) and Bz/Au(111), known as a more strongly bound and a more weakly bound system, respectively.[55] It is well-known that both the Au(111) and Pt(111) surfaces are thermodynamically stable under ambient conditions. The most stable chemisorption site for benzene on Pt(111) is the hollow site, consistent with the results of prior calculations.[53,56] On the Au(111) surface, benzene is mostly physisorbed on the surface.[53] The total energy of the Bz/Au(111) surface for different adsorption sites, on the top, bridge, and hcp-hollow, differ by less than 10 meV, which is also consistent with previous work.[53] For an even comparison with Pt, we place benzene on the hollow site. The average distances between carbon (hydrogen) atoms and Pt atoms at the top layer is 2.19 Å (2.61 Å), which is also consistent with previously reported values.[53,56] For the Au(111) surface, the average distance of carbon and hydrogen atoms from the topmost layer differs by less than 0.01 Å; *i.e.*, the benzene molecule remains flat, with an adsorption height of 3.15 Å. For the chosen adsorption site, the calculated adsorption energy and structural details of the adsorption geometry are given in Table 1.

Table 1. Comparison of the Adsorption Energy (E_{ad}) and Average Normal Distance of Carbon (d_{CM}) and Hydrogen (d_{HM}) Atoms from the Topmost Atomic Layer of the Bz/Pt(111), Bz/Au(111), and Bz/Bi_2Te_3(111) Systems[a]

system	E_{ad} (eV)	d_{CM} (Å)	d_{HM} (Å)
Bz/Pt(111)	−2.25	2.19	2.61
Bz/Au(111)	−0.52	3.14	3.15
Bz/Bi_2Te_3(111)	−0.28	2.96	2.97

[a]The adsorption energy E_{ad} is defined as $E_{ad} = E_{Sys} - E_{Surf} - E_{Mol}$, where Sys, Surf, and Mol refer to the molecule-adsorbed surface, pristine surface, and gas-phase benzene molecule, respectively.

DOI: 10.1021/acs.chemmater.7b03176
Chem. Mater. 2018, 30, 1849–1855

We now turn our attention to the benzene-adsorbed $Bi_2Te_3(111)$ surface. First, in order to identify the surface states of Bi_2Te_3, we consider the pristine surface consisting of four QLs along the (111) direction, with a 1 × 1 unit cell along the *xy* plane. The calculated band structure, including SOC effects, is in good agreement with Figure 2 of ref 52. Generally, the wave function of a surface state decays rapidly inside the bulk. But in the case of a thin TI surface, states emanating from the top and bottom surfaces may couple, leading to an energy gap at the Dirac point. Calculations we performed for $Bi_2Te_3(111)$ surfaces with increasing thickness confirmed that at four QLs the magnitude of this energy gap diminishes practically to zero and the dispersion of the surface bands is essentially saturated (see details given in the Supporting Information), which is in agreement with previously reported first-principles results.[52,57−59] Next, we introduce the benzene molecule to the Bi_2Te_3 surface. The equilibrium distance between benzene and the $Bi_2Te_3(111)$ surface is found to be 2.9 Å. Similar to Bz/Au(111), the distances of different C or H atoms of the benzene molecule and Te atoms at the top layer of the Bi_2Te_3 surface do not differ by more than 0.02 Å from each other. Table 1 lists corresponding values for the Bz/$Bi_2Te_3(111)$ system. Our calculation finds different adsorption sites for the benzene molecule on the Bi_2Te_3 surface to be energetically close (total energy difference between any two adsorption sites of less than 7 meV). In the following, we choose the adsorption site to be on top. The adsorbed molecule is placed such that one Te atom is exactly below the center of the six C atoms of benzene. The adsorption height of the TI is between those on Pt and Au, but the adsorption energy on Bi_2Te_3 is only 0.28 eV, significantly lower than for the metals.

In order to understand these adsorption trends in terms of surface electronic structure, Figure 2 shows the density of states

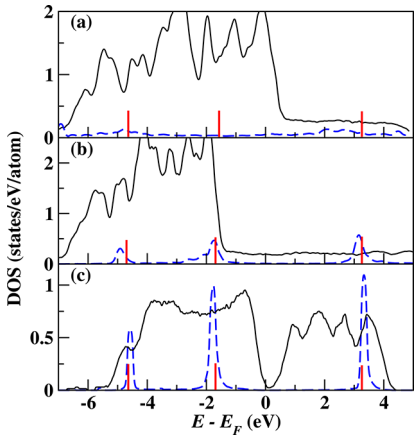

Figure 2. (a) Density of states (DOS) curves projected onto the slab (black solid line) and the carbon π states of the benzene molecule (blue dashed line) adsorbed on the (111) surface of (a) Pt, (b) Au, and (c) Bi_2Te_3. Vertical lines (red) represent the computed π state energy levels of the free benzene molecule. Energies are reported with respect to the Fermi level, E_F.

projected onto the slab and onto the π states of the benzene molecule for all three systems studied here. The computed discrete π-system energy states of the gas-phase benzene molecule, shifted to align with the states of the adsorbed molecule, are also shown for comparison. Note that it is well-known that the PBE functional fails to predict the metal-induced renormalization of the molecular gap, which facilitates the comparison but precludes quantitative determination of level alignment with respect to the Fermi level.[60−64] For Pt, the π-state-projected DOS spreads over a broad range of energy (more than 8 eV) both below and above the Fermi energy, indicating significant hybridization,[65] primarily between Pt d states and benzene π states. It is well-established that in the case of a transition metal surface having partially filled d states, the average energy of the d states relative to the Fermi level is a good measure for the strength of chemisorption.[66] This is reflected in the Bz/Pt(111) system, in which the d bands lying close to the Fermi energy significantly hybridize with the π states of the adsorbed benzene molecule. For Au, however, the molecular resonances broaden with respect to the gas phase but remain relatively narrow in energy. For Bi_2Te_3, the molecular resonances are even narrower, indicating an even smaller perturbation of the molecular electronic structure. This provides clear evidence for chemisorption on the Pt surface, physisorption on the Au surface, and weak physisorption on the Bi_2Te_3 surface. This picture is fully consistent with the above-discussed ordering of the adsorption energies. Furthermore, near the Fermi level, the DOS projected on the d orbitals of the Pt atoms at the top surface, that are closest to the benzene molecule, is lower than the DOS projected on other surface Pt atoms that are farther away from the molecule, indicating hybridization of the former with benzene molecular orbitals. This difference is smaller for Au and virtually zero for the Te atoms at the top of the Bi_2Te_3 surface, again confirming the relative ordering of the adsorption strengths.

To gain further insight into the benzene−TI interaction, we have compared the electronic structure of the molecule-adsorbed surface with that of a structure where the benzene molecule is kept at a large distance (≈ 10 Å) from the surface, such that the molecule−surface interaction is surely negligible. Figure 3 shows the band structure calculated for the two cases (for completeness, a similar comparison for the two metals is given in the Supporting Information). The degeneracy of the top-surface and bottom-surface states crossing the Fermi level around the Γ point is lifted upon benzene adsorption, due to the interaction between the molecule and one of the states of

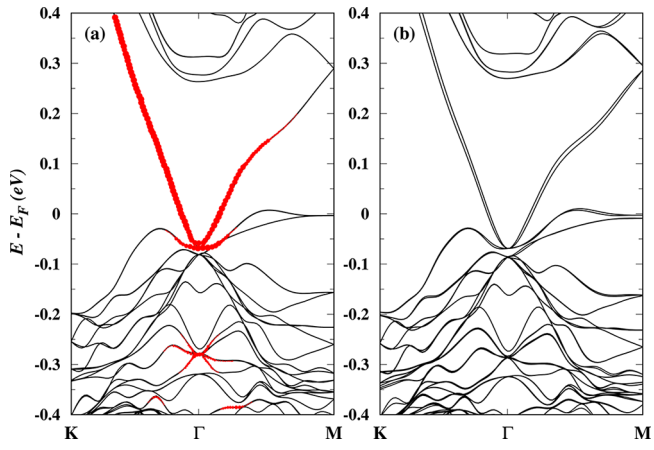

Figure 3. Band structure of a benzene-adsorbed $Bi_2Te_3(111)$ surface for two different adsorbate heights, (a) 10 Å and (b) 2.9 Å. The interaction between the TI surface and the benzene molecule splits the degenerate topological surface states band near the Γ point at the Fermi level. Red circles in panel (a) represent the surface state character of the bands, with radius proportional to the relative surface contribution.

DOI: 10.1021/acs.chemmater.7b03176
Chem. Mater. 2018, 30, 1849−1855

the top surface. Nevertheless, the general nature of the band dispersion around the Fermi energy does not differ substantially, consistent with the topological protection of the surface and the closed-shell molecular electronic structure. We note that for a nearly full-monolayer coverage of the H_2Pc (free-base phthalocyanine) on the Bi_2Se_3 surface, a molecular adsorption height of 2.5 Å and negligible overlap between the frontier orbitals of the molecule and the TI surface have been reported,[32] in agreement with the nature of the results reported here.

A different perspective on the extent of molecule−substrate interaction is given by the spatial distribution of the charge density. This electronic charge distribution around the benzene molecule, projected on the carbon-atom-containing plane of the benzene molecule, for the gas-phase and the three surface-adsorbed molecules, is given in Figure 4. In the figure, isovalue

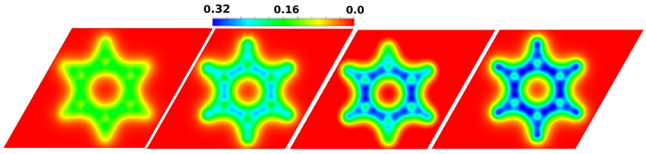

Figure 4. Electronic charge density projected on the carbon-atom-containing plane of the benzene molecule. From left to right, the panels correspond to Bz/Pt(111), Bz/Au(111), Bz/Bi_2Te_3(111), and the gas-phase benzene molecule. The color bar represents iso-surface values (e/Bohr^3) of the charge density.

surfaces of the charge density, for the four cases depicted, are plotted. Clearly, the charge distribution for the Bz/Bi_2Te_3(111) system is very close to that of the gas-phase molecule, indicating weak physisorption. That of Bz/Au(111) exhibits some charge loss to the substrate, in line with stronger physisorption, and that of Bz/Pt(111) exhibits significantly larger charge loss, in line with chemisorption. This trend of relative strength of molecule−substrate interaction is fully consistent with that inferred in Figure 2 from DOS considerations.

Additional insights into the strength and nature of the molecule−substrate interaction can be obtained using a perturbation model, as suggested in ref 67. This model is based on expressing the Hamiltonian of the molecule-adsorbed substrate, H_{ads}, as

$$H_{ads} = H_{iso} + V \tag{1}$$

where H_{iso} is the Hamiltonian of the noninteracting substrate and single molecule (in the same geometry as that of the real system), such that V represents the coupling between the molecule and substrate. Treating V as a perturbation, and assuming that substrate−molecule interaction proceeds mostly via the frontier orbitals of the benzene molecule, second-order perturbation theory yields an approximate expression for the adsorption energy:

$$E_{chem} = \sum_{i=HOMO-n}^{HOMO} \int_{\epsilon_F}^{+\infty} \frac{n_{slab}(\epsilon)|V_{CB}|^2}{\epsilon - \epsilon_{benzene}^{(i)}} d\epsilon + \sum_{i=LUMO}^{LUMO+m} \int_{-\infty}^{\epsilon_F} \frac{n_{slab}(\epsilon)|V_{VB}|^2}{\epsilon_{benzene}^{(i)} - \epsilon} d\epsilon \tag{2}$$

where $n_{slab}(\epsilon)$ is the density of states of the slab model, V_{VB} represents matrix elements of the coupling between valence band states and unoccupied molecular states, V_{CB} represents matrix elements of the coupling between conduction band states and occupied molecular states, $\epsilon_{benzene}^{(i)}$ is the energy of the molecular state, and m (n) corresponds to the number of unoccupied (occupied) states used. Here, we used n = 2 and m = 3, except for the Bz/Au(111) system, where m = 4. The first term in eq 2 corresponds to electron donation from the benzene occupied states to the substrate, and the second term corresponds to back-donation of electrons from the substrate to the benzene unoccupied states.

Adsorption energies of the three substrate−molecule systems, obtained from the perturbation model, are summarized in Table 2. Clearly, the energies predicted from the model

Table 2. Energy Contributions to the Adsorption Energy from a Perturbation Model, in eV[a]

	OCC	UN	total	DFT
Bz/Pt(111)	2.417	0.773	3.190	2.25
Bz/Au(111)	0.009	0.469	0.478	0.52
Bz/Bi_2Te_3(111)	0.197	0.057	0.254	0.28

[a]"OCC" and "UN" represent occupied and unoccupied molecular states states, respectively, corresponding to energy contributions from benzene electron donation and substrate back-donation. "Total" is their sum and "DFT" is the non-perturbative adsorption energy calculated using DFT.

are reasonably close to those obtained from the treatment of the full system. Interestingly, the relative adsorption energy contributions of the Bz/Bi_2Te_3(111) system are qualitatively similar to the Bz/Pt(111) one, with non-negligible donation (larger) and back-donation (smaller) contributions to the adsorption energy, whereas for Bz/Au(111) mainly weak back-donation is observed. Further insight into this behavior is afforded by considering the coupling matrix elements evaluated using the molecular states and substrate states for benzene interacting with the Pt, Au, and Bi_2Te_3 surfaces, as shown in Figure 5. For the Bz/Pt(111) system, strong coupling terms corresponding to both donation and back-donation are found, consistent with the stronger nature of the Pt−benzene interaction. For the Bz/Au(111), however, most of the strong coupling elements are at the lower right corner of Figure 5b, corresponding to weaker back-donation. Most interestingly in our context, for the TI−benzene system, the behavior of the coupling matrix elements is qualitatively very similar to that of Bz/Pt(111), but with much smaller magnitude in terms of energy gain owing to electron transfer, i.e., with much lower chemical interaction (note that the color bar for panel c in Figure 5 represents a smaller range of matrix element magnitudes). The latter is fundamental for understanding surface chemical activity and catalysis.[66] This provides an additional perspective for how the TI metallic states promote the same kind of interaction as that of more reactive metals but will not necessarily be useful toward surface reactivity enhancement as the interaction is very weak.

Finally, we note that in light of the importance of d states in the interaction between benzene and Pt, a topic of interest for further research would be the strength of adsorption of benzene on a TI surface in which the topological band inversion involves d states. We are aware of two recent reports of such TI materials, NaBaBi[68] and $IrBi_3$,[69] showing topological band inversion involving the d state at high pressure. At ambient pressure, however, these compounds either remain in the

DOI: 10.1021/acs.chemmater.7b03176
Chem. Mater. 2018, 30, 1849−1855

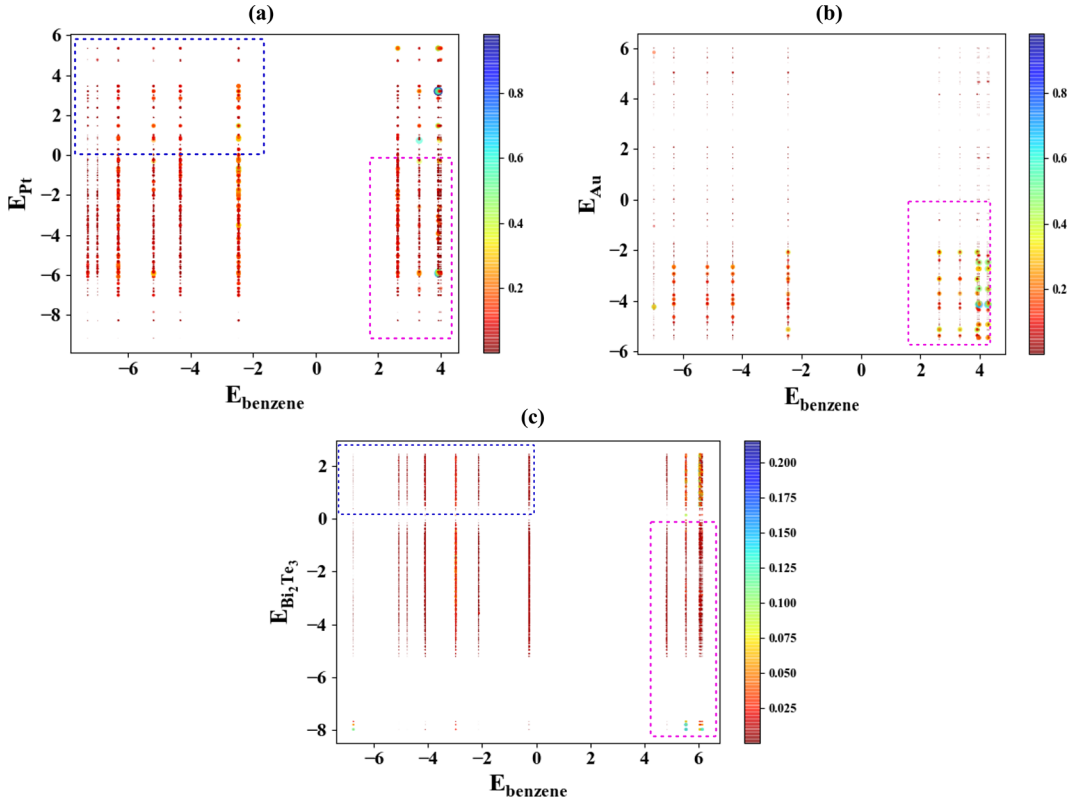

Figure 5. Coupling matrix element magnitudes describing the interaction between a benzene molecule and a (a) Pt(111), (b) Au(111), and (c) Bi_2Te_3(111) substrate. *x* axis: energy of molecular state. *y* axis: energy of substrate state. Color scale: magnitude of the coupling matrix element. Eigenenergies for each substrate and benzene state have been shifted so as to obtain an aligned vacuum level. Zero denotes the position of the Fermi level. The blue and magenta dashed line frames denote molecule donation terms and substrate back-donation terms, respectively. All quantities are in eV.

normal metallic state ($IrBi_3$) or undergo topological band inversion involving p states (NaBaBi).

CONCLUSIONS

In conclusion, we considered benzene adsorbed on three different types of (111) surfaces: Bi_2Te_3, a prototypical example of a three-dimensional TI, and two conventional metals, Pt and Au. We identified clear adsorption trends: chemisorption for Pt, physisorption for Au, and weak physisorption for Bi_2Te_3. This was inferred by combining insights from DFT-based calculations of the adsorption energy, analysis of the density of states, analysis of the charge density corresponding to the molecular π system, and a model calculation based on perturbation theory. Specifically for the TI surface, the result shows that the presence of metallic surface states is not a sufficient condition for surface reactivity. The same methodology can be used to study more complex molecule-adsorbed TI surfaces.

ASSOCIATED CONTENT

Supporting Information

The Supporting Information is available free of charge on the ACS Publications website at DOI: 10.1021/acs.chemmater.7b03176.

Band structure of metallic surfaces with and without adsorption of a benzene molecule, band structure of bulk Bi_2Te_3, and band structure of the Bi_2Te_3(111) surface as a function of thickness (number of quintuple layers) (PDF)

AUTHOR INFORMATION

Corresponding Author

*E-mail: leeor.kronik@weizmann.ac.il.

ORCID

Liang Z. Tan: 0000-0003-4724-6369

Andrew M. Rappe: 0000-0003-4620-6496

Leeor Kronik: 0000-0001-6791-8658

Author Contributions

S.S. and J.Y. contributed equally to this work.

Notes

The authors declare no competing financial interest.

ACKNOWLEDGMENTS

J.Y. and L.Z.T. acknowledge the support of the Department of Energy under grant DE-FG02-07ER15920 and computational support from the NERSC of the DOE. A.M.R. acknowledges support from the National Science Foundation, under grant DMR-1120901. S.S. and L.K. acknowledge the support from the Israel Science Foundation. S.S. acknowledges the Koshland Foundation and McDonald−Leapman grant support.

REFERENCES

(1) Fu, L.; Kane, C. L.; Mele, E. J. Topological insulators in three dimensions. *Phys. Rev. Lett.* **2007**, *98*, 106803.

(2) Fu, L.; Kane, C. L. Topological insulators with inversion symmetry. *Phys. Rev. B: Condens. Matter Mater. Phys.* **2007**, *76*, 045302.

(3) Moore, J. E. The birth of topological insulators. *Nature* **2010**, *464*, 194−198.

DOI: 10.1021/acs.chemmater.7b03176
Chem. Mater. 2018, 30, 1849−1855

(4) Hasan, M. Z.; Kane, C. L. *Colloquium*: Topological insulators. *Rev. Mod. Phys.* **2010**, *82*, 3045−3067.
(5) Qi, X.-L.; Zhang, S.-C. Topological insulators and superconductors. *Rev. Mod. Phys.* **2011**, *83*, 1057−1110.
(6) Müchler, L.; Zhang, H.; Chadov, S.; Yan, B.; Casper, F.; Kübler, J.; Zhang, S.-C.; Felser, C. Topological insulators from a chemist's perspective. *Angew. Chem., Int. Ed.* **2012**, *51*, 7221−7225.
(7) Bansil, A.; Lin, H.; Das, T. *Colloquium*: Topological band theory. *Rev. Mod. Phys.* **2016**, *88*, 021004.
(8) Memmel, N. Monitoring and modifying properties of metal surfaces by electronic surface states. *Surf. Sci. Rep.* **1998**, *32*, 91−163.
(9) Ishii, H.; Sugiyama, K.; Ito, E.; Seki, K. Energy level alignment and interfacial electronic structures at organic/metal and organic/organic interfaces. *Adv. Mater.* **1999**, *11*, 605−625.
(10) Cahen, D.; Kahn, A.; Umbach, E. Energetics of molecular interfaces. *Mater. Today* **2005**, *8*, 32−41.
(11) Barth, J. V. Molecular architectonic on metal surfaces. *Annu. Rev. Phys. Chem.* **2007**, *58*, 375−407.
(12) Tautz, F. S. Structure and bonding of large aromatic molecules on noble metal surfaces: The example of PTCDA. *Prog. Surf. Sci.* **2007**, *82*, 479−520.
(13) Ueno, N.; Kera, S. Electron spectroscopy of functional organic thin films: Deep insights into valence electronic structure in relation to charge transport property. *Prog. Surf. Sci.* **2008**, *83*, 490−557.
(14) Kronik, L.; Koch, N. Electronic properties of organic-based interfaces. *MRS Bull.* **2010**, *35*, 417−421.
(15) Koch, N.; Ueno, N.; Wee, A. T. S. *The Molecule-Metal Interface*; John Wiley & Sons, 2013.
(16) Bocquet, M.-L.; Rappe, A. M.; Dai, H.-L. A density functional theory study of adsorbate-induced work function change and binding energy: Olefins on Ag(111). *Mol. Phys.* **2005**, *103*, 883−890.
(17) Heimel, G.; Rissner, F.; Zojer, E. Modeling the electronic properties of π-conjugated self-assembled monolayers. *Adv. Mater.* **2010**, *22*, 2494−2513.
(18) Natan, A.; Kronik, L.; Haick, H.; Tung, R. T. Electrostatic properties of ideal and non-ideal polar organic monolayers: Implications for electronic devices. *Adv. Mater.* **2007**, *19*, 4103−4117.
(19) Witte, G.; Lukas, S.; Bagus, P. S.; Wöll, C. Vacuum level alignment at organic/metal junctions: Cushion effect and the interface dipole. *Appl. Phys. Lett.* **2005**, *87*, 263502.
(20) Cahen, D.; Naaman, R.; Vager, Z. The cooperative molecular field effect. *Adv. Funct. Mater.* **2005**, *15*, 1571−1578.
(21) Kronik, L.; Morikawa, Y. Understanding the Metal-Molecule Interface from First Principles. In *The Molecule-Metal Interface*; Koch, N., Ueno, N., Wee, A. T. S., Eds.; John Wiley & Sons, 2013; Chapter 3, pp 51−89.
(22) Wang, S.; Wang, W.; Tan, L. Z.; Li, X. G.; Shi, Z.; Kuang, G.; Liu, P. N.; Louie, S. G.; Lin, N. Tuning two-dimensional band structure of Cu(111) surface-state electrons that interplay with artificial supramolecular architectures. *Phys. Rev. B: Condens. Matter Mater. Phys.* **2013**, *88*, 245430.
(23) Lobo-Checa, J.; Matena, M.; Müller, K.; Dil, J. H.; Meier, F.; Gade, L. H.; Jung, T. A.; Stöhr, M. Band formation from coupled quantum dots formed by a nanoporous network on a copper surface. *Science* **2009**, *325*, 300−303.
(24) Temirov, R.; Soubatch, S.; Luican, A.; Tautz, F. S. Free-electron-like dispersion in an organic monolayer film on a metal substrate. *Nature* **2006**, *444*, 350−353.
(25) Romaner, L.; Heimel, G.; Brédas, J.-L.; Gerlach, A.; Schreiber, F.; Johnson, R. L.; Zegenhagen, J.; Duhm, S.; Koch, N.; Zojer, E. Impact of bidirectional charge transfer and molecular distortions on the electronic structure of a metal-organic interface. *Phys. Rev. Lett.* **2007**, *99*, 256801.
(26) Atodiresei, N.; Brede, J.; Lazić, P.; Caciuc, V.; Hoffmann, Ge.; Wiesendanger, R.; Blügel, S. Design of the local spin polarization at the organic-ferromagnetic interface. *Phys. Rev. Lett.* **2010**, *105*, 066601.
(27) Song, Y. R.; Zhang, Y. Y.; Yang, F.; Zhang, K. F.; Liu, C.; Qian, D.; Gao, C. L.; Zhang, S. B.; Jia, J.-F. Magnetic anisotropy of van der Waals absorbed iron (II) phthalocyanine layer on Bi_2Te_3. *Phys. Rev. B: Condens. Matter Mater. Phys.* **2014**, *90*, 180408.
(28) Sessi, P.; Bathon, T.; Kokh, K. A.; Tereshchenko, O. E.; Bode, M. Probing the electronic properties of individual MnPc molecules coupled to topological states. *Nano Lett.* **2014**, *14*, 5092−5096.
(29) Bathon, T.; Sessi, P.; Kokh, K. A.; Tereshchenko, O. E.; Bode, M. Systematics of molecular self-assembled networks at topological insulators surfaces. *Nano Lett.* **2015**, *15*, 2442−2447.
(30) Yang, H.-H.; Chu, Y.-H.; Lu, C.-I.; Butler, C. J.; Sankar, R.; Chou, F.-C.; Lin, M.-T. Organic monolayer protected topological surface state. *Nano Lett.* **2015**, *15*, 6896−6900.
(31) Caputo, M.; Panighel, M.; Lisi, S.; Khalil, L.; Di Santo, G.; Papalaraou, E.; Konczykowski, M.; Krusin-Elbaum, L.; Hruban, A.; Das, P. K.; Fujii, J.; Vobornik, I.; Perfetti, L.; Mugarza, A.; Goldoni, A.; Marsi, M.; et al. Manipulating the topological interface by molecular adsorbates: Adsorption of co-phthalocyanine on Bi_2Se_3. *Nano Lett.* **2016**, *16*, 3409−3414.
(32) Jakobs, S.; Narayan, A.; Stadtmüller, B.; Droghetti, A.; Rungger, I.; Hor, Y. S.; Klyatskaya, S.; Jungkenn, D.; Stöckl, J.; Laux, M.; Monti, O. L. A.; Aeschlimann, M.; Cava, R. J.; Ruben, M.; Mathias, S.; Sanvito, S.; Cinchetti, M. Controlling the spin texture of topological insulators by rational design of organic molecules. *Nano Lett.* **2015**, *15*, 6022−6029.
(33) Wu, L.; Ireland, R. M.; Salehi, M.; Cheng, B.; Koirala, N.; Oh, S.; Katz, H. E.; Armitage, N. P. Tuning and stabilizing topological insulator Bi_2Se_3 in the intrinsic regime by charge extraction with organic overlayers. *Appl. Phys. Lett.* **2016**, *108*, 221603.
(34) Wende, H.; Bernien, M.; Luo, J.; Sorg, C.; Ponpandian, N.; Kurde, J.; Miguel, J.; Piantek, M.; Xu, X.; Eckhold, Ph.; Kuch, W.; Baberschke, K.; Panchmatia, P. M.; Sanyal, B.; Oppeneer, P. M.; Eriksson, O. Substrate-induced magnetic ordering and switching of iron porphyrin molecules. *Nat. Mater.* **2007**, *6*, 516−520.
(35) Brede, J.; Atodiresei, N.; Kuck, S.; Lazić, P.; Caciuc, V.; Morikawa, Y.; Hoffmann, G.; Blügel, S.; Wiesendanger, R. Spin- and energy-dependent tunneling through a single molecule with intramolecular spatial resolution. *Phys. Rev. Lett.* **2010**, *105*, 047204.
(36) Rakhmilevitch, D.; Korytár, R.; Bagrets, A.; Evers, F.; Tal, O. Electron-vibration interaction in the presence of a switchable kondo resonance realized in a molecular junction. *Phys. Rev. Lett.* **2014**, *113*, 236603.
(37) Rakhmilevitch, D.; Sarkar, S.; Bitton, O.; Kronik, L.; Tal, O. Enhanced magnetoresistance in molecular junctions by geometrical optimization of spin-selective orbital hybridization. *Nano Lett.* **2016**, *16*, 1741−1745.
(38) Kong, D.; Cui, Y. Opportunities in chemistry and materials science for topological insulators and their nanostructures. *Nat. Chem.* **2011**, *3*, 845−849.
(39) Chen, H.; Zhu, W.; Xiao, D.; Zhang, Z. Co oxidation facilitated by robust surface states on au-covered topological insulators. *Phys. Rev. Lett.* **2011**, *107*, 056804.
(40) Xiao, J.; Kou, L.; Yam, C.-Y.; Frauenheim, T.; Yan, B. Toward rational design of catalysts supported on a topological insulator substrate. *ACS Catal.* **2015**, *5*, 7063−7067.
(41) Rajamathi, C. R.; Gupta, U.; Pal, K.; Kumar, N.; Yang, H.; Sun, Y.; Shekhar, C.; Yan, B.; Parkin, S.; Waghmare, U. V.; Felser, C.; Rao, C. N. R. Photochemical water splitting by bismuth chalcogenide topological insulators. *ChemPhysChem* **2017**, *18*, 2322−2327.
(42) Perdew, J. P.; Burke, K.; Ernzerhof, M. Generalized gradient approximation made simple. *Phys. Rev. Lett.* **1996**, *77*, 3865.
(43) Ruiz, V. G.; Liu, W.; Zojer, E.; Scheffler, M.; Tkatchenko, A. Density-functional theory with screened van der Waals interactions for the modeling of hybrid inorganic-organic systems. *Phys. Rev. Lett.* **2012**, *108*, 146103.
(44) Tkatchenko, A.; Scheffler, M. Accurate molecular van der Waals interactions from ground-state electron density and free-atom reference data. *Phys. Rev. Lett.* **2009**, *102*, 073005.
(45) Kresse, G.; Furthmüller, J. Efficient iterative schemes for ab initio total-energy calculations using a plane-wave basis set. *Phys. Rev. B: Condens. Matter Mater. Phys.* **1996**, *54*, 11169.

DOI: 10.1021/acs.chemmater.7b03176
Chem. Mater. 2018, 30, 1849−1855

(46) Blöchl, P. E. Projector augmented-wave method. *Phys. Rev. B: Condens. Matter Mater. Phys.* **1994**, *50*, 17953.
(47) Kresse, G.; Joubert, D. From ultrasoft pseudopotentials to the projector augmented-wave method. *Phys. Rev. B: Condens. Matter Mater. Phys.* **1999**, *59*, 1758.
(48) Steiner, S.; Khmelevskyi, S.; Marsmann, M.; Kresse, G. Calculation of the magnetic anisotropy with projected-augmented-wave methodology and the case study of disordered $Fe_{1-x}Co_x$ alloys. *Phys. Rev. B: Condens. Matter Mater. Phys.* **2016**, *93*, 224425.
(49) The surface is grown along the (111) direction of the rhombohedral unit cell of Bi_2Te_3. However, once the 4×4 supercell is formed along the *xy* plane, the normal to the surface is defined as (001) in a hexagonal setting, which is the same as (111) in the rhombohedral unit cell.
(50) Monkhorst, H. J.; Pack, J. D. Special points for Brillouin-zone integrations. *Phys. Rev. B* **1976**, *13*, 5188−5192.
(51) Furthmüller, J.; Hafner, J.; Kresse, G. Dimer reconstruction and electronic surface states on clean and hydrogenated diamond (100) surfaces. *Phys. Rev. B: Condens. Matter Mater. Phys.* **1996**, *53*, 7334−7351.
(52) Park, K.; Heremans, J. J.; Scarola, V. W.; Minic, D. Robustness of topologically protected surface states in layering of Bi_2Te_3 thin films. *Phys. Rev. Lett.* **2010**, *105*, 186801.
(53) Liu, W.; Ruiz, V. G.; Zhang, G.-X.; Santra, B.; Ren, X.; Scheffler, M.; Tkatchenko, A. Structure and energetics of benzene adsorbed on transition-metal surfaces: Density-functional theory with van der Waals interactions including collective substrate response. *New J. Phys.* **2013**, *15*, 053046.
(54) Young, S. M.; Chowdhury, S.; Walter, E. J.; Mele, E. J.; Kane, C. L.; Rappe, A. M. Theoretical investigation of the evolution of the topological phase of Bi_2Se_3 under mechanical strain. *Phys. Rev. B: Condens. Matter Mater. Phys.* **2011**, *84*, 085106.
(55) Liu, W.; Carrasco, J.; Santra, B.; Michaelides, A.; Scheffler, M.; Tkatchenko, A. Benzene adsorbed on metals: Concerted effect of covalency and van der Waals bonding. *Phys. Rev. B: Condens. Matter Mater. Phys.* **2012**, *86*, 245405.
(56) Qi, Y.; Yang, J.; Rappe, A. M. Theoretical modeling of tribochemical reaction on Pt and Au contacts: Mechanical load and catalysis. *ACS Appl. Mater. Interfaces* **2016**, *8*, 7529−7535.
(57) Liu, C.-X.; Zhang, H.; Yan, B.; Qi, X.-L.; Frauenheim, T.; Dai, X.; Fang, Z.; Zhang, S.-C. Oscillatory crossover from two-dimensional to three-dimensional topological insulators. *Phys. Rev. B: Condens. Matter Mater. Phys.* **2010**, *81*, 041307.
(58) Yazyev, O. V.; Moore, J. E.; Louie, S. G. Spin polarization and transport of surface states in the topological insulators Bi_2Se_3 and Bi_2Te_3 from first principles. *Phys. Rev. Lett.* **2010**, *105*, 266806.
(59) Förster, T.; Krüger, P.; Rohlfing, M. *GW* calculations for Bi_2Te_3 and Sb_2Se_3 thin films: Electronic and topological properties. *Phys. Rev. B: Condens. Matter Mater. Phys.* **2016**, *93*, 205442.
(60) Neaton, J. B.; Hybertsen, M. S.; Louie, S. G. Renormalization of molecular electronic levels at metal-molecule interfaces. *Phys. Rev. Lett.* **2006**, *97*, 216405.
(61) Garcia-Lastra, J. M.; Rostgaard, C.; Rubio, A.; Thygesen, K. S. Polarization-induced renormalization of molecular levels at metallic and semiconducting surfaces. *Phys. Rev. B: Condens. Matter Mater. Phys.* **2009**, *80*, 245427.
(62) Thygesen, K. S.; Rubio, A. Renormalization of molecular quasiparticle levels at metal-molecule interfaces: Trends across binding regimes. *Phys. Rev. Lett.* **2009**, *102*, 046802.
(63) Biller, A.; Tamblyn, I.; Neaton, J. B.; Kronik, L. Electronic level alignment at a metal-molecule interface from a short-range hybrid functional. *J. Chem. Phys.* **2011**, *135*, 164706.
(64) Egger, D. A.; Liu, Z.-F.; Neaton, J. B.; Kronik, L. Reliable energy level alignment at physisorbed molecule-metal interfaces from density functional theory. *Nano Lett.* **2015**, *15*, 2448−2455.
(65) Morin, C.; Simon, D.; Sautet, P. Chemisorption of Benzene on Pt(111), Pd(111), and Rh(111) metal surfaces: A structural and vibrational comparison from first principles. *J. Phys. Chem. B* **2004**, *108*, 5653−5665.
(66) Nørskov, J. K.; Abild-Pedersen, F.; Studt, F.; Bligaard, T. Density functional theory in surface chemistry and catalysis. *Proc. Natl. Acad. Sci. U. S. A.* **2011**, *108*, 937−943.
(67) Cooper, V. R.; Kolpak, A. M.; Yourdshahyan, Y.; Rappe, A. M. Supported metal electronic structure: Implications for molecular adsorption. *Phys. Rev. B: Condens. Matter Mater. Phys.* **2005**, *72*, 081409.
(68) Sun, Y.; Wang, Q.-Z.; Wu, S.-C.; Felser, C.; Liu, C.-X.; Yan, B. Pressure-induced topological insulator in NaBaBi with right-handed surface spin texture. *Phys. Rev. B: Condens. Matter Mater. Phys.* **2016**, *93*, 205303.
(69) Yang, M.; Liu, W.-M. The d-p band-inversion topological insulator in bismuth-based skutterudites. *Sci. Rep.* **2015**, *4*, 5131.

DOI: 10.1021/acs.chemmater.7b03176
Chem. Mater. 2018, 30, 1849−1855